Neuroradiology (1995) 37: 356–361
© Springer-Verlag 1995

I. Yamada
S. Suzuki
Y. Matsushima

Moyamoya disease: diagnostic accuracy of MRI

Received: 9 February 1994
Accepted: 31 March 1994

I. Yamada (✉) · S. Suzuki
Department of Radiology,
Faculty of Medicine,
Tokyo Medical and Dental University,
1-5-45 Yushima, Bunkyo-ku,
Tokyo 113, Japan

Y. Matsushima
Department of Neurosurgery,
Faculty of Medicine,
Tokyo Medical and Dental University,
Tokyo, Japan

Abstract Our purpose was to evaluate the diagnostic accuracy of MRI in moyamoya disease. We studied 30 patients with this disease, comparing MRI and angiographic findings. The diagnostic value of MRI was evaluated for occlusive lesions, collateral vessels, and parenchymal lesions. In all patients bilateral occlusion or stenosis of the supraclinoid internal carotid artery and proximal anterior and middle cerebral arteries was clearly shown by MRI, and staging of the extent of occlusion agreed with angiographic staging in 44 (73 %) of 60 arteries. MRI, particularly coronal images, clearly showed basal cerebral moyamoya vessels in 54 hemispheres, and 45 of a total of 71 large leptomeningeal and transdural collateral vessels were identified. MRI also showed parenchymal lesions in 48 (80 %) hemispheres, and the extent of occlusion in the anterior and posterior circulations respectively correlated with white matter and cortical and/or subcortical infarcts.

Key words Moyamoya disease · Magnetic resonance imaging · Cerebral angiography

Introduction

Moyamoya disease, a rare cerebrovascular occlusive disease of unknown cause, is commonly seen in Japan [1–3], but has also been reported elsewhere [4, 5]. Angiography reveals the following characteristics: bilateral occlusion or stenosis primarily involving the supraclinoid portion of the internal carotid artery (ICA) and extending to the proximal portions of the anterior (ACA) and middle (MCA) cerebral arteries, and parenchymal, leptomeningeal, and transdural collateral vessels which supply the ischaemic brain [6–8].

MRI may be employed to investigate moyamoya disease, since it provides vascular information without use of contrast medium [9]. We reported the usefulness and limitations of MR angiography (MRA) in moyamoya disease [10]. To our knowledge, no report has appeared dealing with the diagnostic accuracy of MRI in a large number of cases of moyamoya disease, although MRI is used more commonly than MRA. We therefore undertook to evaluate the accuracy of MRI in moyamoya disease.

Materials and methods

We studied 30 patients with moyamoya disease by MRI. These were consecutive cases, confirmed as moyamoya disease by cerebral angiography, 11 males and 19 females, whose age at the time of examination ranged from 6 months to 54 years (average 14 ± 12 years). Age at the onset of symptoms ranged from 3 months to 47 years (average 9 ± 12 years), the average interval from the appearance of the first symptoms to examination being about 5 years. There were 27 patients who had not had surgery; 3 had undergone an external carotid artery to ICA bypass.

MRI was performed with a 1.5-T system and a circularly polarised quadrature head coil which operated in transmitting and receiving modes. In all patients, axial and coronal T1-weighted spin-echo (SE) images were obtained with a 600/20 sequence (repetition time/echo time ms) and two signals averaged. Axial proton-density- and T2-weighted images were obtained as a SE 3000/20, 80 sequence with one signal average. All images were acquired with field of view 20 cm, matrix 256 × 256, and section thickness 5 mm with a 1-mm intersection gap. Axial T1-, proton-

Table 1 MRI and angiographic staging of the ICA bifurcation

MRI stage (number)	Angiographic stage (number)				
	1 (2)	2 (18)	3 (13)	4 (18)	5 (9)
1 (2)	2	0	0	0	0
2 (8)	0	8	0	0	0
3 (12)	0	5	7	0	0
4 (27)	0	5	4	18	0
5 (11)	0	0	2	0	9

Table 2 MRI and angiographic demonstration of moyamoya vessels

MRI (number)	Angiography (number)			
	None (3)	Slight (14)	Moderate (13)	Marked (30)
None (6)	3	3	0	0
Slight (11)	0	11	0	0
Moderate (17)	0	0	13	4
Marked (26)	0	0	0	26

density-, and T2-weighted images were obtained of the whole brain, and coronal T-weighted images from the genu to the splenium of the corpus callosum were obtained.

All patients also underwent transfemoral cerebral angiography, including bilateral internal and external carotid and unilateral or bilateral vertebral artery injections. This was performed within 1 month of the MRI, after which the findings were reviewed and used as the standard of reference in analysing the MRI studies. The latter were interpreted without knowledge of the angiographic findings.

Using a method reported previously [11], we classified the ICA bifurcation – according to the degree of stenosis in the supraclinoid portion of the ICA and the proximal portions of the ACA and MCA – into one of the following stages: 1, slight to moderate stenosis of ICA bifurcation (lumen $\geqq$ 10 % of normal); 2, severe stenosis of the bifurcation (lumen < 10 % of normal); 3, occlusion of the ACA or MCA; 4, occlusion of the ICA or the ACA and MCA, with partial retention of the ACA or MCA trunk; and 5, occlusion of the ICA or the ACA and MCA, with no demonstration of the ACA and MCA main trunk.

Finally, we classified the abnormal basal cerebral moyamoya vessels (MMV) into four grades: none, slight, moderate, or marked.

Results

The MRI findings are summarised in Tables 1–4. The images were reviewed for occlusive lesions, collateral vessels, and parenchymal lesions, and were compared lesion by lesion with the angiograms.

Table 4 Occlusive lesions of the PCA on angiography and cerebral infarcts on MRI

Infarcts (number)	Angiographic PCA lesions (number)			
	Normal (43)	Stenosis (5)	Occlusion (12)	*P*
Cortical or subcortical (17)	4 (9 %)	3 (60 %)	10 (83 %)	< 0.001
White matter (44)	30 (70 %)	5 (100 %)	9 (75 %)	Not significant

Occlusive lesions

In all patients, occlusion or stenosis of the supraclinoid portion of the ICA and the proximal portions of the ACA and MCA was detected bilaterally (Figs. 1, 2). Of the 60 supraclinoid ICAs, 52 (87 %) were assessed accurately with MRI, but in 8 the extent of occlusive disease was overestimated (Fig. 3). For 60 ACAs, MCAs and posterior cerebral arteries (PCAs), the corresponding figures were 46 (77 %), 51 (85 %) and 54 (90 %) accurately assessed, with 14, 9 and 6 in which the extent of occlusive disease was overestimated.

In 44 (73 %) of the 60 ICA bifurcations, staging of the occlusive lesions by MRI correlated well with angiographic staging (Table 1). However, the stage as determined with MRI was higher than the angiographic stage in 16: from stage 2 to stage 3 in five arteries, from stage 2 to stage 4 in another five, from stage 3 to stage 4 in four, and from stage 3 to stage 5 in two.

Collateral vessels

Basal cerebral MMV were shown by MRI in 54 cerebral hemispheres (Figs. 1, 4). The coronal images in particular clearly revealed their full extent, from the chiasmatic cistern to the basal ganglia and the deep white matter. Furthermore, in 53 (88 %) of the 60 cerebral hemispheres, the MRI grade of MMV correlated well with the grade determined by angiography (Table 2). However, MRI failed to show MMV in three hemispheres and led to underestimation of their extent in four.

Table 3 Angiographic staging of ICA bifurcation and cerebral infarcts on MRI

Infarcts (number)	Angiographic stage (number)					
	1 (2)	2 (18)	3 (13)	4 (18)	5 (9)	*P*
White matter (44)	0 (0 %)	12 (67 %)	10 (77 %)	14 (78 %)	8 (89 %)	< 0.05
Cortical or subcortical (17)	0 (0 %)	4 (22 %)	6 (46 %)	5 (28 %)	2 (22 %)	Not significant

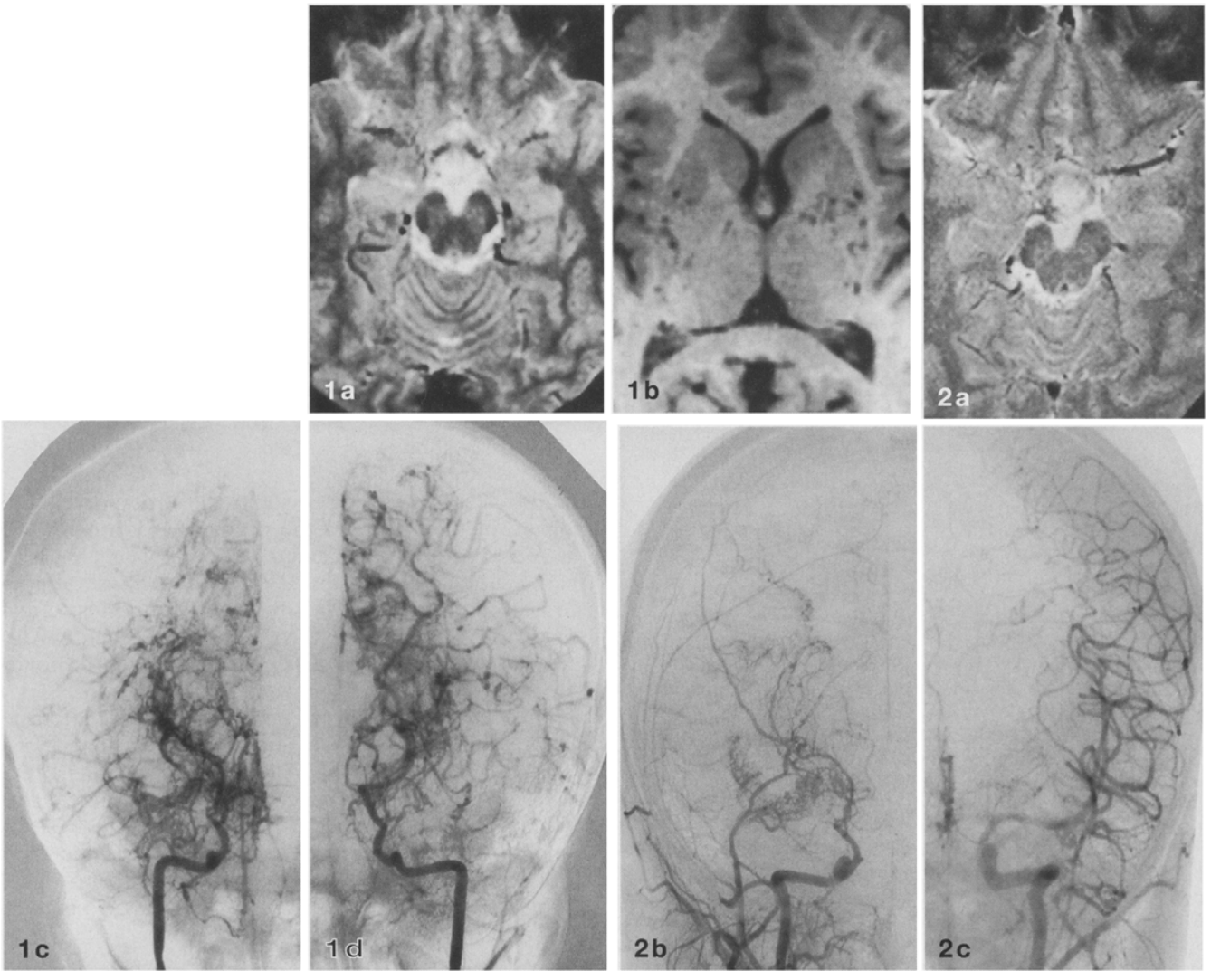

Fig. 1a–d A 7-year-old boy. **a** Axial T2-weighted image shows that the supraclinoid ICA and proximal ACA and MCA are occluded bilaterally. **b** Axial T1-weighted image shows marked bilateral moyamoya vessels (MMV). **c,d** Right and left internal carotid arteriography, frontal projection, show that both ICA are occluded in the distal supraclinoid portion and the ACA and MCA in their proximal portions. Marked MMV are seen

Fig. 2a–c A 9-year-old boy. **a** Axial T2-weighted image shows that the right ICA, ACA, and MCA are completely occluded and the proximal left ACA is stenotic, although the proximal MCA is normal in calibre. **b** Right internal carotid arteriogram, frontal projection, shows that the ICA is occluded in its distal supraclinoid portion and the ACA and MCA in their proximal portions. Moderate MMV are seen. **c** Left internal carotid arteriogram shows that the proximal ACA is so stenotic that its branches are poorly seen, although the proximal MCA and the supraclinoid ICA are normal in calibre

Leptomeningeal anastomoses from posterior to anterior circulations were shown well by MRI in 40 cerebral hemispheres (Fig. 5). In six hemispheres, however, no such anastomoses were identified. Transdural collateral vessels were observed on MRI in five cerebral hemispheres. In four hemispheres, where there had been bypass surgery, the collateral vessels from the dilated superficial temporal artery to the territory of the MCA were seen (Fig. 6). However, in 20 hemispheres, no transdural collateral vessels were detected.

Parenchymal lesions

Parenchymal lesions were shown by MRI in 48 (80 %) cerebral hemispheres. White matter infarcts, the most frequent, were seen in 44 hemispheres (73 %). Cortical and/or subcortical infarcts were seen as 21 lesions in 17 hemispheres (28 %), including 6 haemorrhagic in-

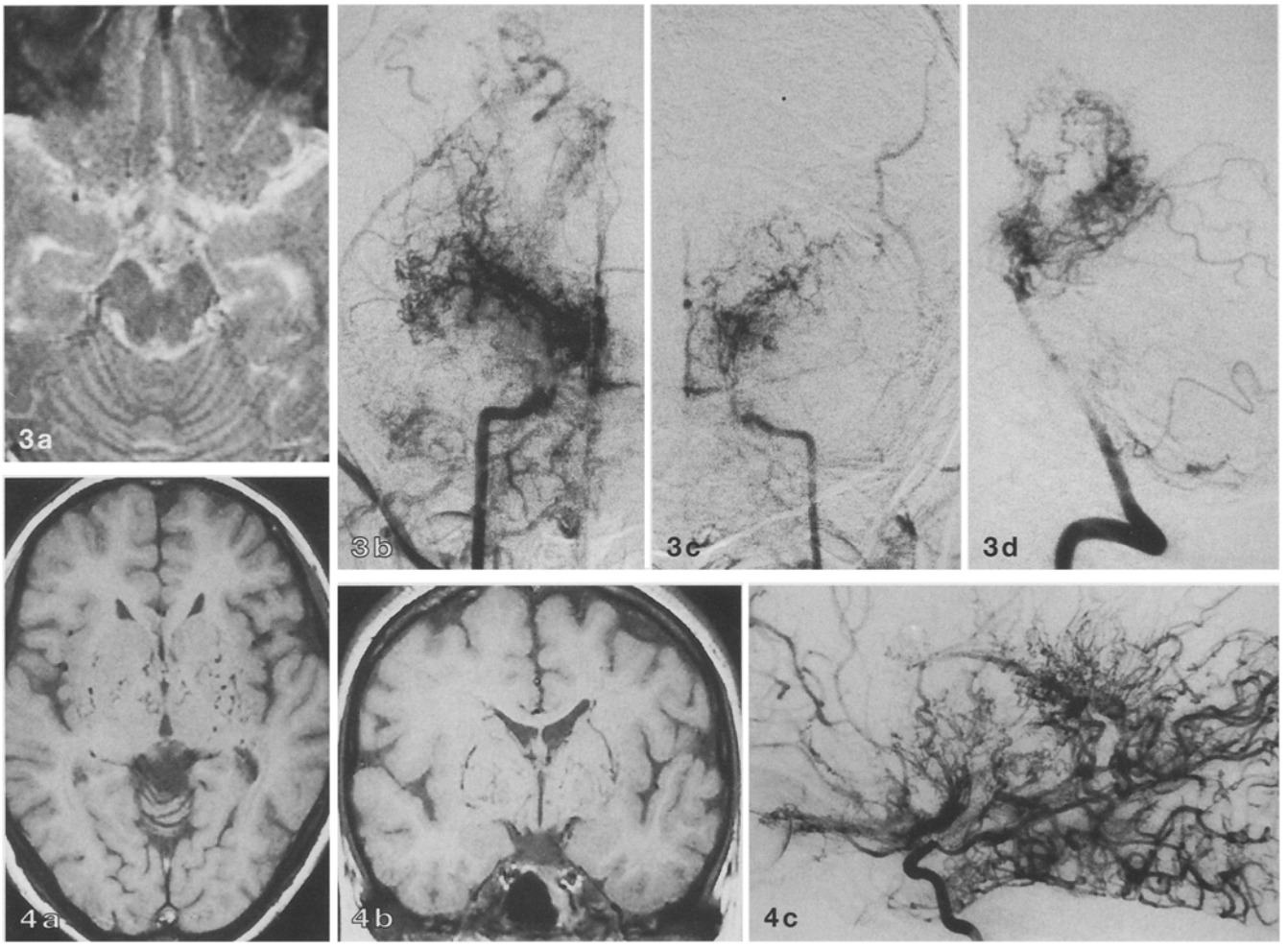

Fig. 3a–d A 13-year-old girl. **a** Axial T2-weighted image shows that the supraclinoid ICA and the proximal ACA, MCA and PCA are occluded bilaterally. **b** Right internal carotid arteriogram, frontal projection, shows that the ICA is occluded in its distal supraclinoid portion and the ACA and MCA in their proximal portions. Marked MMV are seen. **c** Left internal carotid arteriogram, frontal projection, shows that the supraclinoid ICA and the proximal ACA and MCA are markedly stenotic. Moderate MMV are seen. **d** Left vertebral arteriogram, lateral projection, shows that both PCA are occluded proximally. Marked MMV are seen

Fig. 4a–c A 12-year-old girl. **a,b** Axial and coronal T1-weighted images show marked MMV bilaterally. The coronal image shows the full extent of MMV from the chiasmatic cistern to the basal ganglia and deep white matter. **c** Right internal carotid arteriogram, lateral projection, shows that the ICA is occluded in its distal supraclinoid portion. Marked MMV extend from the chiasmatic cistern, and the medullary arteries of the deep white matter are seen. The left internal carotid arteriogram was similar

farcts; signs of cerebral haemorrhage were observed in three hemispheres (5 %). Atrophy was seen in seven hemispheres (12 %), and ventricular dilatation in two (3 %).

The frequency of white matter infarcts increased significantly as the angiographic stage of ICA bifurcation stenosis advanced ($P < 0.05$, Spearman's rank correlation test) (Table 3). Similarly the frequency of cortical and/or subcortical infarcts increased as the PCA stenosis advanced ($P < 0.001$, chi-square test) (Table 4). All examples of cerebral atrophy and ventricular dilatation, except for one of atrophy, were seen in hemispheres with a PCA occlusion ($P < 0.001$ and $P < 0.05$, respectively, chi-square test).

Discussion

Although CT, MRI, and MRA have been reported for the diagnosis of moyamoya disease, angiography is still considered necessary for a definitive diagnosis [9, 10, 12].

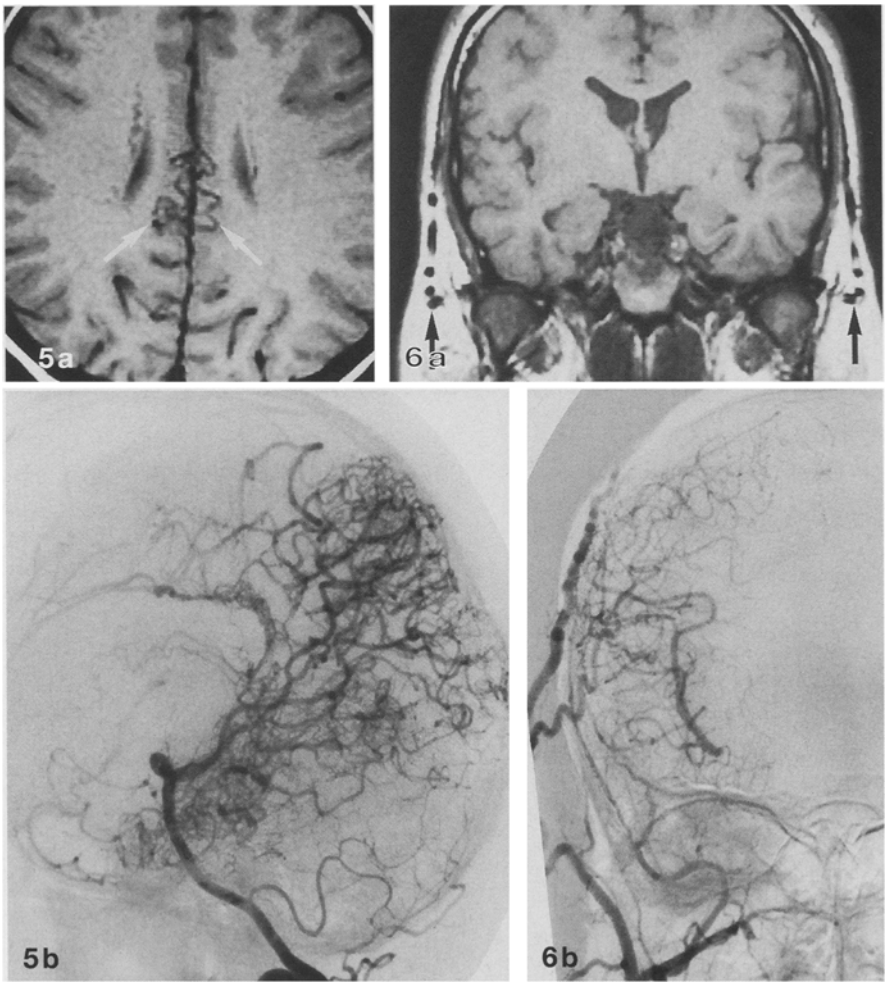

Fig. 5a,b A 10-year-old boy. **a** Axial T1-weighted image shows leptomeningeal collateral vessels *(arrows)* from the PCA branches to the ACA territory in the medial part of both cerebral hemispheres. **b** Left vertebral arteriogram, lateral projection, shows the branches of both PCA to the markedly enlarged and to send leptomeningeal collateral vessels to the ACA territory

Fig. 6a,b A 20-year-old man who had undergone bypass surgery. **a** Coronal T1-weighted image shows that both superficial temporal arteries *(arrows)* are markedly enlarged and send transdural collateral vessels. **b** Right external carotid arteriogram, frontal projection, shows that the superficial temporal artery is markedly enlarged and that the Sylvian branches of the MCA fill via transdural collateral vessels

We have shown that MRI is moderately successful in demonstrating occlusive disease in the basal portions of the ICA, ACA, MCA, and PCA, and that staging of ICA bifurcation lesions by MRI agreed with angiographic staging in 73 % of 60 arteries. However, on MRI stenosis tends to look more severe than on angiography. Detection of bilateral occlusive lesions of the ICA bifurcation is essential for definitive diagnosis of moyamoya disease [6–8].

MRI also performed moderately well in assessment of collateral vessels. In a four-tier system used to grade MMV, the grades determined by MRI and by angiography agreed in 88 % of 60 cerebral hemispheres. Coronal images clearly showed the full extent of MMV involvement. Asari et al. [13] also reported that coronal CT was useful in revealing MMV in the basal ganglia. However, MRI showed only the larger leptomeningeal and transdural collateral vessels. Generally, the extent of small collateral vessels tended to be underestimated.

MRI revealed parenchymal lesions in 80 % of the cerebral hemispheres of patients with moyamoya disease. The frequency of white matter infarcts increased significantly as ICA bifurcation stenosis advanced, and that of cortical and/or subcortical infarcts as PCA stenosis advanced. Since the PCA sends numerous leptomeningeal anastomoses to the anterior circulation, occlusion of the PCA appears to cause severe ischaemia, particularly in the cortical and/or subcortical region. Recent reports have shown that the extent of cerebral infarcts in moyamoya disease affects the response to an external carotid artery to ICA bypass [14, 15]. Thus, the use of MRI for precise assessment of infarcts and other parenchymal lesions could be helpful in assessing the neurological prognosis of patients with moyamoya disease.

We reported the usefulness and limitations of MRA in the diagnosis of moyamoya disease [10]. Staging of stenotic lesions with MRA correlated with conventional angiographic staging in 75 % of cases, and in 75 % the MRA grade of MMV agreed with that of MMV seen on conventional angiography. MRI (88 %) was therefore superior to MRA (75 %) for showing MMV, and slightly

inferior (73 %) to MRA (75 %) for stenotic lesions. We therefore believe that MRI and MRA are complementary in the diagnosis of moyamoya disease. Another strength of MRI is its ability to show parenchymal lesions.

As moyamoya disease advances, stenotic lesions progress, which makes the MMV and parenchymal lesions change [16]. MRI, which can show both vascular and parenchymal lesions, therefore appears suitable for follow-up of patients with moyamoya disease, as well as for initial diagnosis.

Acknowledgement We thank Yasushi Annaka, RT, for his technical contributions and assistance.

References

1. Kudo T (1968) Spontaneous occlusion of the circle of Willis. Neurology 18: 485–496
2. Nishimoto A, Takeuchi S (1968) Abnormal cerebrovascular network related to the internal carotid arteries. J Neurosurg 29: 255–260
3. Suzuki J, Takaku A (1969) Cerebrovascular "moyamoya" disease: disease showing abnormal net-like vessels in base of brain. Arch Neurol 20: 288–299
4. Taveras JM (1969) Multiple progressive intracranial arterial occlusions: a syndrome of children and young adults. AJR 106: 235–268
5. Pecker J, Simon J, Guy G, Herry JF (1973) Nishimoto's disease: significance of its angiographic appearances. Neuroradiology 5: 223–230
6. Handa J, Handa H (1972) Progressive cerebral arterial occlusive disease: analysis of 27 cases. Neuroradiology 3: 119–133
7. Takahashi M (1980) Magnification angiography in moyamoya disease: new observations on collateral vessels. Radiology 136: 379–386
8. Hasuo K, Tamura S, Kudo S, Uchino A, Carlos R, Matsushima T, Kurokawa T, Kitamura K, Matsuura K (1985) Moyamoya disease: use of digital subtraction angiography in its diagnosis. Radiology 157: 107–111
9. Fujisawa I, Asato R, Nishimura K, Togashi K, Itoh K, Noma S, Sagoh T, Minami S, Nakano Y, Yonekawa Y, Torizuka K (1987) Moyamoya disease: MR imaging. Radiology 164: 103–105
10. Yamada I, Matsushima Y, Suzuki S (1992) Moyamoya disease: diagnosis with three-dimensional time-of-flight MR angiography. Radiology 184: 773–778
11. Satoh S, Shibuya H, Matsushima Y, Suzuki S (1988) Analysis of the angiographic findings in cases of childhood moyamoya disease. Neuroradiology 30: 111–119
12. Takahashi M, Miyauchi T, Kowada M (1980) Computed tomography of moyamoya disease: demonstration of occluded arteries and collateral vessels as important diagnostic signs. Radiology 134: 671–676
13. Asari S, Satoh T, Sakurai M, Yamamoto Y, Sadamoto K (1982) The advantages of coronal scanning in cerebral computed angiotomography for diagnosis of moyamoya disease. Radiology 145: 709–711
14. Yamada I, Matsushima Y, Suzuki S (1992) Childhood moyamoya disease before and after encephalo-duro-arterio-synangiosis: an angiographic study. Neuroradiology 34: 318–322
15. Miyamoto S, Kikuchi H, Karasawa J, Nagata I, Ikota T, Takeuchi S (1984) Study of the posterior circulation in moyamoya disease: clinical and neuroradiological evaluation. J Neurosurg 61: 1032–1037
16. Suzuki J, Kodama N (1983) Moyamoya disease: a review. Stroke 14: 104–109